

The Fate of Entanglement

Gilles Perez^{1,2} and William Witczak-Krempa^{1,2,3}

¹*Département de Physique, Université de Montréal, Montréal, QC H3C 3J7, Canada*

²*Centre de Recherches Mathématiques,
Université de Montréal, Montréal, QC H3C 3J7, Canada*

³*Institut Courtois, Université de Montréal, Montréal, QC H2V 0B3, Canada*

Quantum entanglement is a fundamentally non-local correlation between particles. In its simplest realisation, a measurement on one particle is affected by a prior measurement on its partner, irrespective of their separation. For multiple particles, purely collective types of entanglement exist but their detection, even theoretically, remains an outstanding open question. Here, we show that all forms of multi-party entanglement entirely disappear during the typical evolution of a system as it heats up, evolves in time, or as its parts become separated. These results follow from the nature of the entanglement-free continent in the space of physical states, and hold in great generality. We illustrate these phenomena with a frustrated molecular quantum magnet in and out of equilibrium. In contrast, if the particles are fermions, such as electrons, another notion of entanglement exists that precludes entanglement-free regions, and thus protects quantum correlations. These findings provide fundamental knowledge about the structure of entanglement in quantum matter and architectures, paving the way for its manipulation.

Introduction.— Entanglement is a non-local quantum correlation between two or more particles that makes it possible for a measurement on a subset of particles to affect subsequent measurements on the other particles. The effect of the initial measurement is instantaneous, even if the particles are distant. Entanglement not only constitutes a fundamental property of nature, but it is also a resource to perform tasks that would prove impossible without it such as teleportation [1], or more broadly quantum computation [2]. This has driven the community to devise methods to detect and quantify entanglement [3]. Unfortunately, it is not known how to determine with certainty whether a general system is entangled, except in very simple situations such as with 2 qubits. One can better grasp the

complexity of the task by observing that entanglement can exist between more than two parties. In fact, some systems possess 3-party entanglement but no 2-party entanglement of any sort. In this work, we find criteria for such collective non-local quantum correlations in physical systems under very general conditions. For instance, at what temperatures can multi-party entanglement of a given kind exist? We begin by explaining important properties about the space of physical states, and how these determine the fate of entanglement under the evolution of a system with temperature, time or separation. We then illustrate these results with a simple yet generic model: the anti-ferromagnetic Ising model on an icosahedral molecule. Finally, we discuss the fate of entanglement for fermionic systems, where the parity superselection rule greatly modifies the geometry of the space of states and the structure of entanglement.

Separable continent.— We investigate multi-party entanglement of states with m subsystems, as illustrated in Fig. 1a. We shall argue that the end point of the evolution typically corresponds to an un-entangled state, which is called separable. The simplest separable state for a system of m parties is a product,

$$\rho_{\text{prod}} = \rho_1 \otimes \rho_2 \otimes \cdots \otimes \rho_m, \quad (1)$$

where ρ_j is a physical density matrix for subsystem j . The set of separable states is convex [3], namely states composed of a mixture of product states, $\rho_{\text{sep}} = \sum_k p_k \rho_{\text{prod}}^{(k)}$ with $p_k \geq 0$, are also un-entangled. In the space of all physical states, separable ones thus form a separable continent surrounded by an ocean of entangled states, see Fig. 1b. Highly-entangled states live in the deep-blue waters, whereas in the center of the separable continent lies the maximally-mixed state, i.e., the most classical state obtained in the limit of infinite temperature.

We describe the system's state by $\rho(s)$, where s parametrizes the evolution; the final state is $\rho_f \equiv \rho(\infty)$. We shall argue that in situations of physical relevance the final state is generically separable. Moreover, ρ_f typically lies in the interior of the separable continent, not on its frontier. We thus arrive at our main conclusion: the system irreversibly loses all forms of multi-party entanglement beyond some stage in the evolution, as shown in Fig. 1b. Moreover, before reaching land, the system navigates shallow waters, leading to a rapid decimation of entanglement. During this stage one has an effectively separable state. This constitutes a point of significant importance in real-world applications since

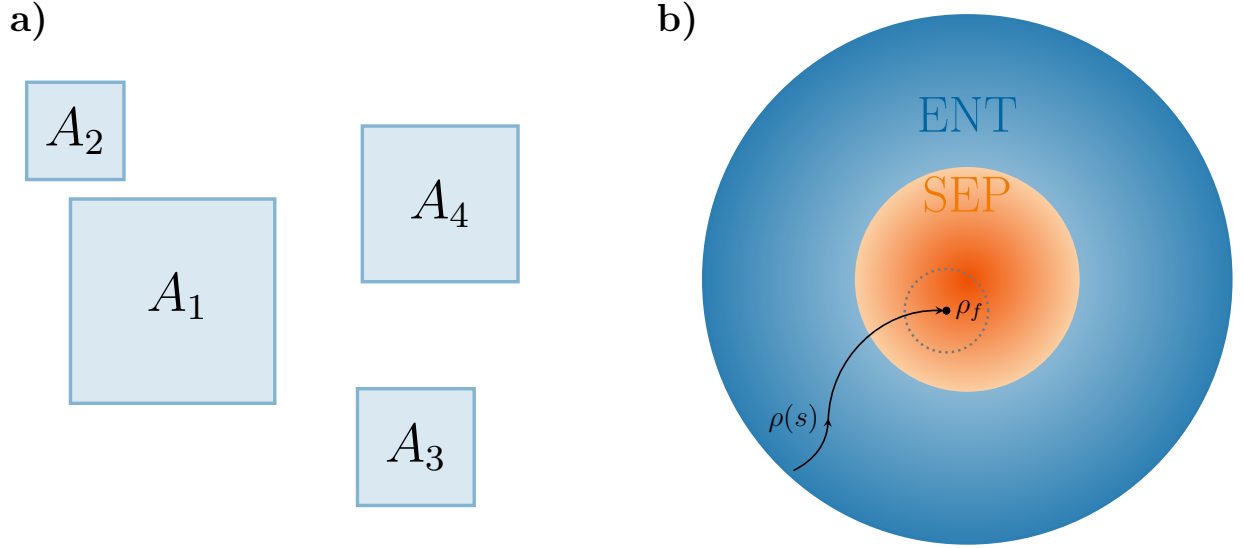


FIG. 1. **Evolution of multi-party entanglement.** **a)** We consider a general state of m subsystems, here illustrated for $m = 4$, which can be in contact with an environment. **b)** The state is described by a density matrix $\rho(s)$ that evolves according to a parameter s such as temperature, time or separation. The blue region represents the sea of entangled states, where deep-blue regions are more entangled than light-blue ones. The orange disk is the separable continent.

determining when a state reaches a very low degree of entanglement is easier than showing exact separability. Nevertheless, we can exploit a mathematical result that tells us when a state is in the interior of the separable continent [4–7]. In the simplest version, the theorem states that a product state (1) lies in the interior if it has full rank, i.e., none of its eigenvalues vanishes. This is coherent with what is known for pure product states: these have minimal rank (a single non-zero eigenvalue), and indeed live on the frontier of the continent as arbitrarily weak perturbations can make them entangled. Furthermore, the argument gives us the radius of a ball in the space of states that lies entirely on the separable continent; this is represented by the dashed line in Fig. 1b. The radius of the ball is proportional to the smallest eigenvalue of the state [7], $R_m = 2^{1-m/2} \lambda_{\min}$. Here, we use the standard notion of distance between two quantum states given by the Frobenius norm: $d(\rho, \rho') = \sqrt{\text{Tr}(\rho - \rho')^2}$. A more general version of the result holds for a mixture of product states with a least one having full rank [7].

Temperature.— In the first application, we take the parameter s to represent the temperature T . Naturally, a very large temperature destroys entanglement, yielding a max-

imally uncorrelated state. The infinite-temperature end point is a full-rank product state, $\rho_f = D^{-1}\mathbb{I}$, where \mathbb{I} represents the identity matrix in the D -dimensional space of the system. This state is located at the center of the separable continent. Hence, there exists a threshold temperature T_m at which we can rigorously conclude that all forms of entanglement between the m subsystems disappear. The minimal eigenvalue of ρ_f being $1/D$, one can readily obtain a temperature above which entanglement is lost. However, in the example below we shall see that the system rapidly enters shallow waters, and becomes effectively separable at much lower temperatures. Sudden death of bipartite entanglement at finite temperature has been observed in different physical systems [8–12].

Time.— In a dynamical situation, the parameter s is the time t , and the final state is the state at $t = \infty$. If ρ_f is on the separable continent, one can conclude that there is a sudden-death time t_m^* at which all m -party entanglement is lost. As the structure of the final state depends on the type of dynamical evolution under study, let us describe an important case in more detail: a quantum quench. One prepares a closed system to be in an eigenstate of a given Hamiltonian H_I , and at some time the Hamiltonian is abruptly changed to a different one, H , resulting in non-trivial time evolution. We then study the state of a subset A of the entire system: the m -party state $\rho(t)$ is obtained by partially tracing over the unobserved part, B . When A is small compared to its complement B , the state is expected to effectively thermalize at large times. As discussed above, temperature tends to destroy entanglement, which leads to the expectation that numerous quench protocols will land on the continent.

We can argue in full generality that the entanglement dynamics after a quench from a pure product state typically follows a rise-and-fall behavior. For early times, we consider the evolution of the system with parameter $s = t^{-1}$. The “final” state of this evolution is the initial state of the quench, namely a pure product state with rank one, i.e., not full rank. As we previously discussed, such states lie on the boundary, or the shore, of the separable continent. Therefore, there is no entanglement sudden death in this evolution. Looking back at the quench protocol with time as the parameter, this implies that entanglement is generated at $t = 0^+$ after the quench. As discussed above, at late times the state typically lands on the continent, or in very shallow waters at a finite time, yielding an entanglement sudden death or strong suppression. These early- and late-time behaviors result in the rise-and-fall dynamics of entanglement. Such behavior has been observed for simple entanglement measures in numerous systems [13–19].

Space.— We now study the fate of entanglement as a function of the separation between the m subsystems by scaling their separations by λ , which parametrizes the evolution. At large λ , in a local physical system the state will factorise into a product form, where the description of each subsystem becomes independent, since all correlations become suppressed at large separations. If the asymptotic product state is of full rank, there exists a critical scale beyond which all entanglement vanishes. An important application is to study the entanglement between m subsystems embedded in a larger system as these are chosen to be progressively further apart. The state at infinite λ satisfies the product form, Eq. (1), where ρ_j is the reduced density matrix of subsystem j obtained by tracing out the complementary degrees of freedom. Let us take the entire system to be in equilibrium at a temperature $T \geq 0$. At large separation, the state of subsystem A_1 is given by $\rho_1 = \text{Tr}_{A_2 \dots A_m B} \sum_n p_n |E_n\rangle\langle E_n|$, where we have traced over the environment B , and the $(m-1)$ subsystems A_j . The sum runs over all eigenstates of the Hamiltonian. The thermal Boltzmann probabilities are $p_n = e^{-E_n/T}/\mathcal{Z}$. We now need to determine whether ρ_1 has full rank. Let us first examine the restriction of the eigenstates of the Hamiltonian to A_1 , $\rho_1^{(n)} = \text{Tr}_{A_2 \dots A_m B} |E_n\rangle\langle E_n|$. From the point of view of A_1 , the degrees of freedom in B act as a bath, thus introducing statistical randomness in $\rho_1^{(n)}$. Since we take A_1 to be sufficiently small compared to the complement, the bath generically has sufficient resources to induce statistical fluctuations that span the entire Hilbert space of A_1 . Such ergodicity implies that $\rho_1^{(n)}$ will be of full rank. This indeed occurs for the majority of eigenstates as they live near the middle of the energy spectrum. The eigenstate thermalization hypothesis [20–22] then states that the reduced density matrix on A_1 is approximately thermal, with the temperature determined by the energy E_n . The approximately thermal density matrix, obtained by restricting the Hamiltonian to A_1 , then has full rank. Our statement, which we call the *full-rank hypothesis* (FRH), is more general: *all* eigenstates of a generic local Hamiltonian have a full-rank reduced density matrix associated with a sufficiently small subregion. In practice, the subregion should not exceed half the system.

Now, the reduced density matrix of subsystem 1 is the convex sum $\rho_1 = \sum_n p_n \rho_1^{(n)}$. The FRH implies that ρ_1 inherits full rank from the states $\rho_1^{(n)}$. (Since the sum of a full-rank matrix and an arbitrary one also has full rank, we actually only need to know that at least one $\rho_1^{(n)}$ is of full rank.) As the same holds for the other subsystems, we conclude that the $\lambda = \infty$ product has full rank, and thus lies on the separable continent. Therefore,

there exists a scale beyond which all entanglement disappears. The sudden death occurs irrespective of the number of subsystems or the precise nature of the state; it even holds at a quantum critical phase transition where quantum fluctuations proliferate to all scales. This result shows that, although local observables can possess slowly decaying algebraic correlations, entanglement decays drastically faster, to the point of having a finite range. Our conclusion encompasses and generalises numerous examples of bipartite entanglement sudden death at finite separation [23–29], which are very specific cases of the general multi-party phenomenon.

Icosahedral molecule.— We illustrate the above results with a simple quantum system: the anti-ferromagnetic Ising model on the 12-spin icosahedron, see Fig. 2a, with Hamiltonian $H = J \sum_{\text{bonds } \langle i,j \rangle} \sigma_i^x \sigma_j^x - h \sum_{\text{sites } i} \sigma_i^z$. The first term corresponds to an anti-ferromagnetic interaction $J > 0$ that tends to anti-align neighbouring spins along x , while the second one is a transverse field that polarises all spins along z . Such a molecular quantum magnet is a combination of identical triangular faces, and thus possesses strong geometric frustration. In what follows we shall measure energy in units of the exchange coupling by setting $J = 1$. We investigate the fate of 2- and 3-spin entanglement as a function of magnetic field, temperature, time a separation by considering three distinct quantities. See the Supplemental Material (SM) for their precise definitions. First, we compute a measure of 2-party entanglement, focusing on a pair of adjacent spins, called the logarithmic negativity \mathcal{E} [30, 31]. In the case of two spins, $\mathcal{E} = 0$ implies that the reduced density matrix is separable [32], whereas for entangled states we have $\mathcal{E} > 0$. Second, we study the 3-spin entanglement on a triangular face of the molecule via the geometric entanglement \mathcal{D} [3] defined as the smallest distance between the state and the separable continent,

$$\mathcal{D} = \min_{\rho_{\text{sep}}} d(\rho, \rho_{\text{sep}}), \quad (2)$$

where the minimisation is over all ρ_{sep} living on the continent. This powerful measure detects all forms of entanglement. Finally, we employ a criterion W that indicates the presence of genuine 3-party entanglement when $W > 0$ [33]. This type of entanglement relates all three parties, and cannot be described in term 2-party entanglement. When $W = 0$, a definitive conclusion cannot be made. We note that both \mathcal{D} and W require a minimisation procedure in a multi-parameter space, making their evaluation more demanding than simpler measures such as \mathcal{E} . As a prerequisite, we checked that the FRH holds for subregions of adjacent spins

with 1, 2 and 3 sites by obtaining the 2^{12} eigenstates via exact numerical diagonalization, see SM.

We first consider the fate of entanglement with varying magnetic field at zero temperature, so that the evolution is parameterized by $s = h$, see Fig. 2b. At $h = 0$, the 2-spin reduced density matrix is a full-rank separable state, implying the existence of a value $h_2^* > 0$ of the field below which the state is separable, and hence $\mathcal{E}(h < h_2^*) = 0$. We find $h_2^* \approx 0.6$. In contrast, the 3-spin reduced density matrix is not separable at small h and we have $\mathcal{D} > 0$. In the opposite limit of $h \rightarrow \infty$, the system becomes fully polarized and is in a pure product state. Both 2- and 3-spins density matrices are thus pure product states, i.e., of rank one, and lie on the shore of the separable continent. Entanglement therefore decreases with increasing h but does not experience a sudden death. These features are clearly visible in Fig. 2b. In the following we focus on the case $h = 3$, where 2-party and genuine 3-party entanglement are present at zero temperature. For additional data regarding the phase diagram of the model, see SM.

Let us now investigate the fate of entanglement with temperature at $h = 3$. From the criterion of the separable ball around the infinite-temperature state [7], we determine the temperatures where m -party entanglement is guaranteed to be absent for $m = 2, 3$. We find $T_2 = 8$ and $T_3 = 22$, respectively. However, these do not tell us if entanglement is absent at lower temperatures. The logarithmic negativity \mathcal{E} and the criterion W vanish at temperatures $T_{\mathcal{E}} = 2.1$ and $T_W = 1.5$, which are much smaller than T_2 and T_3 . Finally, we observe that for $T_3^* \approx 3$, the geometric entanglement \mathcal{D} is of order 10^{-4} , and further rapidly decreases with temperature beyond that point. Hence, the 3-spin density matrix is essentially separable for temperatures much smaller than the rigorous bound T_3 . We report these results in Fig. 2c.

Next, we consider the evolution of entanglement with time during a quantum quench. We initialise the system in a pure product state of up and down spins in the σ^z -basis at $t = 0$, and let it evolve under the Ising Hamiltonian discussed above with $h = 3$, see SM for details regarding the initial state. In Fig. 2d we show the evolution of our three measures of interest. Both \mathcal{E} and W rapidly rise, reach a maximum, and fall to zero, with W being the shortest lived. We thus see a clear illustration of the sudden death of entanglement for the case of $m = 2$ spins. The distance \mathcal{D} follows the same behavior but displays small oscillations close to zero for later times. The state quickly reaches the shallow waters around $t_3^* \approx 0.4$,

while an exact sudden death does not occur for $m = 3$, presumably due to the small size of the molecule. An interesting observation is that the non-equilibrium evolution can generate stronger 2- and 3-party entanglement compared to what is found in equilibrium, even at zero temperature, see Fig. 2c. Finally, we observe qualitatively identical behavior for other initial conditions.

As a final example, we consider the evolution of entanglement with separation, working in the groundstate at $h = 3$. First, for $m = 2$ spins, we find that entanglement disappears when the spins become separated by 2 bonds. Second, for $m = 3$ spins, we scale the minimal triangle by $\lambda = 2$ so that the sides have bond-length two. In that case we have $W = 0$, and we find that the state is extremely close to a separable one, $\mathcal{D} = \mathcal{O}(10^{-6})$, which is many orders of magnitude smaller than for the adjacent triangle.

No continent for fermions.— The above discussion holds for systems of quantum spins. Crucially, spin operators at different sites are independent (they commute with each other) because they represent bosons. However, there exist other particles in nature that do not commute, instead they acquire a minus sign upon exchange: fermions, like electrons or protons. Individual fermion operators possess this relative non-locality with other fermions, but observers nevertheless witness a local world since physical operators are made of an even number of fermions, and are thus bosonic. The density matrix of a physical fermionic system made of m subsystems thus possesses even fermion parity. But how does fermion parity affects the definition of entanglement by constraining viable separable states? A natural notion follows from declaring that a fermionic m -party state is un-entangled if it can be written as $\rho_{\text{sep}}^F = \sum_k p_k \rho_1^{(k)} \otimes \rho_2^{(k)} \otimes \cdots \otimes \rho_m^{(k)}$, where each $\rho_j^{(k)}$ has even parity and the p_k form a probability distribution [34–36]. This definition guarantees that the state has no quantum correlations among the m components, and can thus be prepared locally. Certain states can be brought to this form, but where some $\rho_j^{(k)}$ do not have even parity. These states cannot be prepared locally and their non-local correlations can be exploited for quantum tasks such as quantum teleportation or quantum data hiding [37–39].

Given an un-entangled fermionic physical state ρ_{sep}^F , can we find an entanglement-free region around it as was the case for bosons? We show that the answer is no, and then discuss the consequences. The argument, as given in Ref. [40], is the following. It suffices to consider the case with $m = 2$ components by performing a small deformation, $\rho_{\text{sep}}^F + \delta\rho$, where $\delta\rho$ has zero trace and contains terms of odd fermion parity for subsystem 1. For example, one can

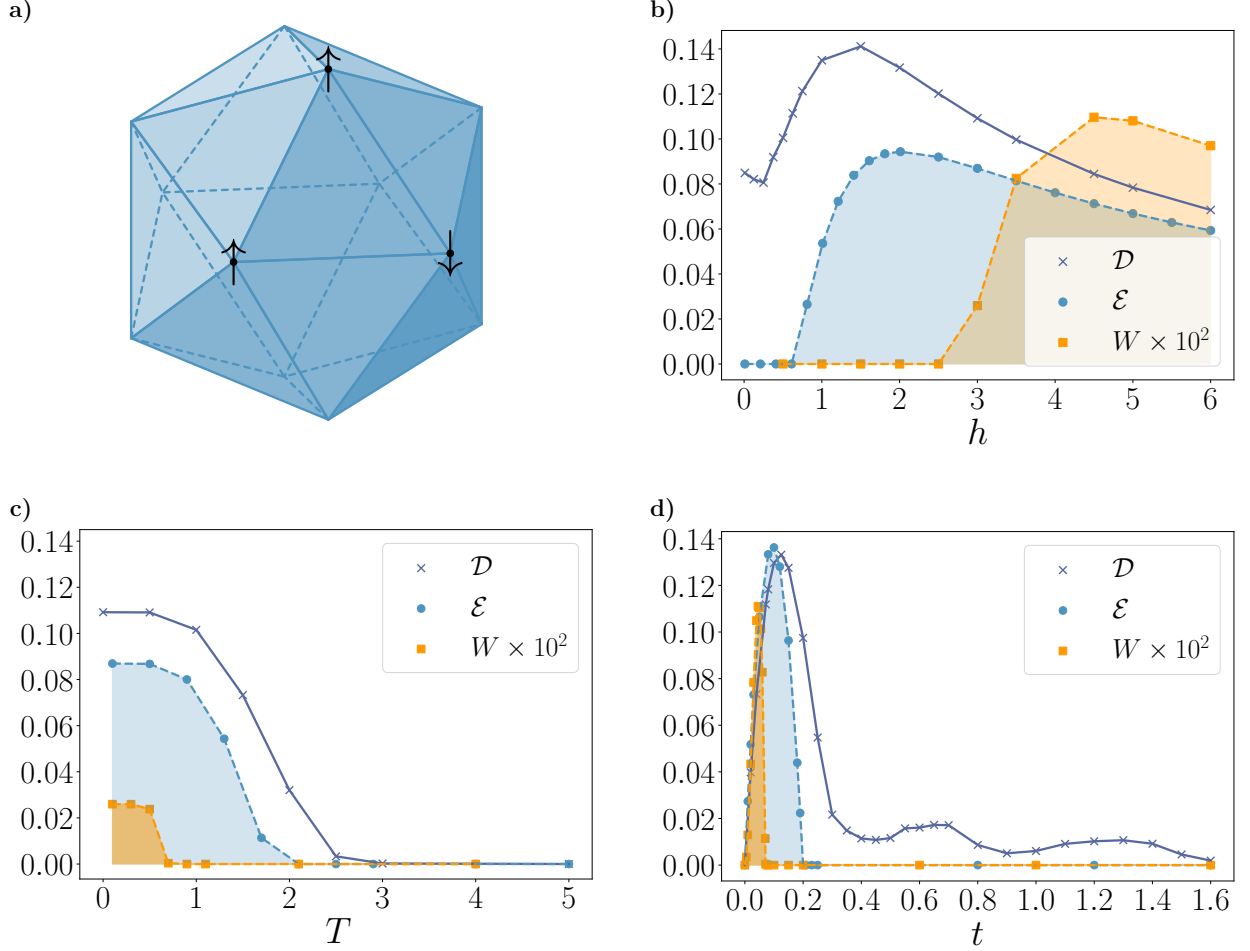


FIG. 2. **Icosahedral molecule and its entanglement evolutions.** **a)** Illustration of the quantum molecular magnet with icosahedral geometry. **b)** Dependence of the geometric entanglement \mathcal{D} , the 2-spin logarithmic negativity \mathcal{E} and the genuine 3-party entanglement criterion W in the icosahedral molecule as a function of the transverse field at zero temperature. **c)** Evolution of the same quantities as a function of temperature with $h = 3$. **d)** Same quantities as a function of time in a quench protocol where the system is prepared in a product state and evolves under the anti-ferromagnetic Ising Hamiltonian with $h = 3$.

hop an odd number of fermions between subsystems 1 and 2, e.g., $\delta\rho = \epsilon(|01\rangle\langle 10| + |10\rangle\langle 01|)$ with positive $\epsilon \ll 1$. The deformed state does not have even parity for subsystem 1, and hence is not separable, even for arbitrarily small ϵ . Therefore, no entanglement-free region exists around a fermionic separable state since nearby states arbitrarily close to ρ_{sep}^F contain entanglement between any two subsystems. In the fermionic world, there is thus no separable

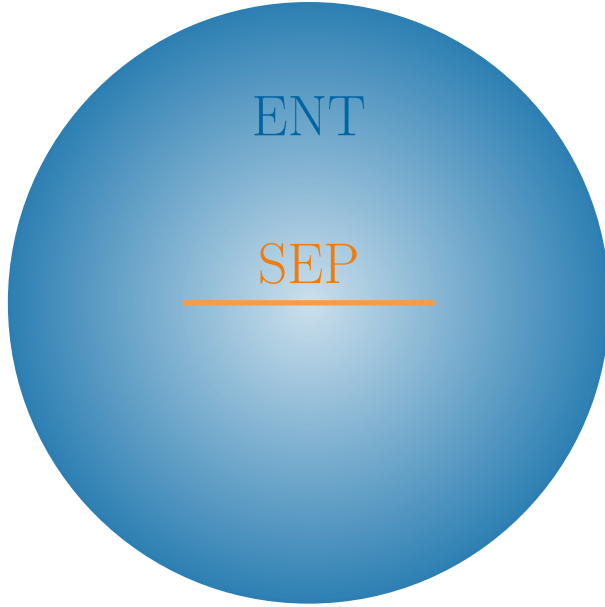


FIG. 3. **Structure of the space of states for fermions.** For fermions, because of the fermion-parity superselection rule, there is no separable continent. Instead, separable states form a zero-width sand beach with entangled states arbitrarily close.

continent. Separable states lie on a zero-width sand beach, surrounded by an ocean of entangled states arbitrarily close by. We illustrate this in Fig 3.

Turning the tables around, fermionic entanglement is more robust since the state cannot land on a continent upon evolution. Let us say that we heat a fermion system that contains multi-party entanglement at low T . The infinite temperature state is un-entangled, but entanglement will decay gradually as a function of temperature without a sudden death. This behavior was observed for integer quantum Hall states [41] and free-fermion systems [34, 42]. Analogous conclusions hold for temporal or spatial evolution. For instance, the entanglement between disjoint regions in fermionic conformal field theories in arbitrary dimensions decays as a power-law with the distance, without a sudden death [29].

The geometry of the space of states acquires a distinct structure due to the presence of a superselection rule, which is due to the fermion parity symmetry. By the same argument, a similar structure arises with other superselection rules, where a symmetry becomes enforced. Requiring the symmetry to hold for subsystems constrains states that can appear in separable decompositions, thus leading to the disappearance of separable continents. Symmetry-enforced entanglement is thus more resilient.

Outlook.— In this paper, we discussed how the structure of the space of physical states, and in particular the presence of a separable continent, leads to the sharp disappearance of entanglement in various physical situations, under very generic assumptions. For fermionic systems, the parity superselection rule forbids the existence of the separable continent and drastically modifies the fate of entanglement. In particular, fermionic systems do not experience entanglement sudden death, in stark contrast with bosonic ones. Interestingly, the same conclusion holds for other types of superselection rules, providing a generic recipe for the creation of robust entangled states.

These new insights regarding the structure of entanglement in many-body states will have strong impact for quantum simulation and computation. For instance, efficient algorithms used to simulate quantum matter should incorporate the fact that distant particles are not entangled in spin/boson systems, which strongly constrains the variational space of many-body wave functions. Our work also paves the way for numerous outstanding research avenues. For instance, it will be essential to investigate how multi-party entanglement evolves in a plethora of realistic model Hamiltonians, and to determine the criteria that govern its demise under evolution. We have also seen examples of how quantum matter out-of-equilibrium generates stronger multi-party entanglement than in equilibrium. This is the tip of iceberg: we expect that non-equilibrium dynamics can lead to rich entanglement structures that await to be discovered.

Acknowledgements.— G.P. holds an FRQNT Postdoctoral Fellowship, and acknowledges support from the Mathematical Physics Laboratory of the Centre de Recherches Mathématiques (CRM). W.W.-K. is supported by a grant from the Fondation Courtois, a Chair of the Institut Courtois, a Discovery Grant from NSERC, and a Canada Research Chair.

-
- [1] C. H. Bennett, G. Brassard, C. Crépeau, R. Jozsa, A. Peres, and W. K. Wootters, “Teleporting an unknown quantum state via dual classical and Einstein-Podolsky-Rosen channels,” *Phys. Rev. Lett.* **70**, 1895 (1993).
 - [2] M. A. Nielsen and I. L. Chuang, *Quantum computation and quantum information*. Cambridge University Press, 2010.

- [3] V. Vedral, M. B. Plenio, M. A. Rippin, and P. L. Knight, “Quantifying entanglement,” *Phys. Rev. Lett.* **78**, 2275 (1997).
- [4] S. L. Braunstein, C. M. Caves, R. Jozsa, N. Linden, S. Popescu, and R. Schack, “Separability of very noisy mixed states and implications for NMR quantum computing,” *Phys. Rev. Lett.* **83**, 1054 (1999).
- [5] L. Gurvits and H. Barnum, “Largest separable balls around the maximally mixed bipartite quantum state,” *Phys. Rev. A* **66**, 062311 (2002).
- [6] S.-Q. Shen, M. Li, and L. Li, “A bipartite separable ball and its applications,” *J. Phys. A: Math. Theor.* **48**, 095302 (2015).
- [7] R. Y. Wen and A. Kempf, “Separable ball around any full-rank multipartite product state,” *J. Phys. A: Math. Theor.* **56**, 335302 (2023).
- [8] M. C. Arnesen, S. Bose, and V. Vedral, “Natural thermal and magnetic entanglement in the 1D Heisenberg model,” *Phys. Rev. Lett.* **87**, 017901 (2001).
- [9] J. Anders, “Thermal state entanglement in harmonic lattices,” *Phys. Rev. A* **77**, 062102 (2008).
- [10] S.-S. Gong and G. Su, “Thermal entanglement in one-dimensional Heisenberg quantum spin chains under magnetic fields,” *Phys. Rev. A* **80**, 012323 (2009).
- [11] O. Hart and C. Castelnovo, “Entanglement negativity and sudden death in the toric code at finite temperature,” *Phys. Rev. B* **97**, 144410 (2018).
- [12] Z. Ma, C. Han, Y. Meir, and E. Sela, “Symmetric inseparability and number entanglement in charge-conserving mixed states,” *Phys. Rev. A* **105**, 042416 (2022).
- [13] T. Yu and J. H. Eberly, “Sudden death of entanglement,” *Science* **323**, 598 (2009).
- [14] J. Ma, Z. Sun, X. Wang, and F. Nori, “Entanglement dynamics of two qubits in a common bath,” *Phys. Rev. A* **85**, 062323 (2012).
- [15] V. Alba and P. Calabrese, “Quantum information dynamics in multipartite integrable systems,” *EPL* **126**, 60001 (2019).
- [16] S. Murciano, V. Alba, and P. Calabrese, “Quench dynamics of Rényi negativities and the quasiparticle picture,” in *Entanglement in Spin Chains: From Theory to Quantum Technology Applications*, p. 397. 2022.
- [17] G. Perez, R. Bonsignori, and P. Calabrese, “Dynamics of charge-imbalance-resolved entanglement negativity after a quench in a free-fermion model,” *J. Stat. Mech.* 053103

- (2022).
- [18] G. Perez and R. Bonsignori, “Analytical results for the entanglement dynamics of disjoint blocks in the XY spin chain,” *J. Phys. A: Math. Theor.* **55**, 505005 (2023).
 - [19] S. Sang, Z. Li, T. H. Hsieh, and B. Yoshida, “Ultrafast entanglement dynamics in monitored quantum circuits,” *PRX Quantum* **4**, 040332 (2023).
 - [20] J. M. Deutsch, “Quantum statistical mechanics in a closed system,” *Phys. Rev. A* **43**, 2046 (1991).
 - [21] M. Srednicki, “Chaos and quantum thermalization,” *Phys. Rev. E* **50**, 888 (1994).
 - [22] M. Rigol, V. Dunjko, and M. Olshanii, “Thermalization and its mechanism for generic isolated quantum systems,” *Nature* **452**, 854 (2008).
 - [23] A. Osterloh, L. Amico, G. Falci, and R. Fazio, “Scaling of entanglement close to a quantum phase transition,” *Nature* **416**, 608 (2002).
 - [24] T. J. Osborne and M. A. Nielsen, “Entanglement in a simple quantum phase transition,” *Phys. Rev. A* **66**, 032110 (2002).
 - [25] Y. Javanmard, D. Trapin, S. Bera, J. H. Bardarson, and M. Heyl, “Sharp entanglement thresholds in the logarithmic negativity of disjoint blocks in the transverse-field Ising chain,” *New J. Phys.* **20**, 083032 (2018).
 - [26] N. Klco and M. J. Savage, “Entanglement spheres and a UV-IR connection in effective field theories,” *Phys. Rev. Lett.* **127**, 211602 (2021).
 - [27] N. Klco and M. J. Savage, “Geometric quantum information structure in quantum fields and their lattice simulation,” *Phys. Rev. D* **103**, 065007 (2021).
 - [28] G. Perez, C. Berthiere, and W. Witczak-Krempa, “Separability and entanglement of resonating valence-bond states,” *SciPost Phys.* **15**, 066 (2023).
 - [29] G. Perez and W. Witczak-Krempa, “Are fermionic conformal field theories more entangled?,” [arXiv:2310.15273](https://arxiv.org/abs/2310.15273).
 - [30] G. Vidal and R. F. Werner, “Computable measure of entanglement,” *Phys. Rev. A* **65**, 032314 (2002).
 - [31] M. B. Plenio, “Logarithmic negativity: a full entanglement monotone that is not convex,” *Phys. Rev. Lett.* **95**, 090503 (2005).
 - [32] M. Horodecki, P. Horodecki, and R. Horodecki, “Separability of mixed states: necessary and sufficient conditions,” *Phys. Lett. A* **223**, 1 (1996).

- [33] O. Gühne and M. Seevinck, “Separability criteria for genuine multiparticle entanglement,” *New J. Phys.* **12**, 053002 (2010).
- [34] M.-C. Banuls, J. I. Cirac, and M. M. Wolf, “Entanglement in fermionic systems,” *Phys. Rev. A* **76**, 022311 (2007).
- [35] C. Spee, K. Schwaiger, G. Giedke, and B. Kraus, “Mode entanglement of Gaussian fermionic states,” *Phys. Rev. A* **97**, 042325 (2018).
- [36] H. Shapourian and S. Ryu, “Entanglement negativity of fermions: Monotonicity, separability criterion, and classification of few-mode states,” *Phys. Rev. A* **99**, 022310 (2019).
- [37] F. Verstraete and J. I. Cirac, “Quantum nonlocality in the presence of superselection rules and data hiding protocols,” *Phys. Rev. Lett.* **91**, 010404 (2003).
- [38] N. Schuch, F. Verstraete, and J. I. Cirac, “Nonlocal resources in the presence of superselection rules,” *Phys. Rev. Lett.* **92**, 087904 (2004).
- [39] N. Schuch, F. Verstraete, and J. I. Cirac, “Quantum entanglement theory in the presence of superselection rules,” *Phys. Rev. A* **70**, 042310 (2004).
- [40] F. Benatti, R. Floreanini, and U. Marzolino, “Entanglement in fermion systems and quantum metrology,” *Phys. Rev. A* **89**, 032326 (2014).
- [41] C.-C. Liu, J. Geoffrion, and W. Witczak-Krempa, “Entanglement negativity versus mutual information in the quantum Hall effect and beyond,” [arXiv:2208.12819](#).
- [42] W. Choi, M. Knap, and F. Pollmann, “Finite Temperature Entanglement Negativity of Fermionic Symmetry Protected Topological Phases and Quantum Critical Points in One Dimension,” [arXiv:2310.20566](#).
- [43] A. Peres, “Separability criterion for density matrices,” *Phys. Rev. Lett.* **77**, 1413 (1996).

Supplemental Material: The Fate of Entanglement

Gilles Perez^{1,2} and William Witczak-Krempa^{1,2,3}

¹*Département de Physique, Université de Montréal, Montréal, QC H3C 3J7, Canada*

²*Centre de Recherches Mathématiques,*

Université de Montréal, Montréal, QC H3C 3J7, Canada

³*Institut Courtois, Université de Montréal, Montréal, QC H2V 0B3, Canada*

A. ENTANGLEMENT MEASURES AND CRITERIA

We give the definitions of the entanglement-related quantities we discuss in the main text, namely the logarithmic negativity \mathcal{E} , the geometric entanglement \mathcal{D} and the genuine 3-party entanglement criterion W .

Logarithmic negativity

We consider the density matrix ρ matrix pertaining to two subsystems 1 and 2. The logarithmic negativity [30, 31] is

$$\mathcal{E} = \log \|\rho^{T_1}\| \quad (\text{S1})$$

where $\|X\| = \text{Tr} \sqrt{XX^\dagger}$ is the trace-norm, and ρ^{T_1} is the partially-transposed density matrix with respect to subsystem 1. This entanglement measure is related to the Peres separability criterion for density matrices [43]. In full generality, a vanishing logarithmic negativity is only a necessary condition for separability, but in the case of two spins (or qubits), it is both necessary and sufficient [32].

Geometric entanglement

The geometric entanglement [3] is the distance between the state ρ and the closest separable state,

$$\mathcal{D} = \min_{\rho_{\text{sep}}} \sqrt{\text{Tr}(\rho - \rho_{\text{sep}})^2}. \quad (\text{S2})$$

Numerically, we choose a number of product states (up to 7) in the convex combination, and optimize the distance function over these separable states.

Genuine 3-party entanglement criterion

The criterion W is defined from the matrix elements ρ_{ij} , $i, j = 1, \dots, 8$, of a 3-spin density matrix. It reads [33]

$$W = |\rho_{23}| + |\rho_{25}| + |\rho_{35}| - \sqrt{\rho_{11}\rho_{44}} - \sqrt{\rho_{11}\rho_{66}} - \sqrt{\rho_{11}\rho_{77}} - \frac{1}{2}(\rho_{22} + \rho_{33} + \rho_{55}). \quad (\text{S3})$$

Positive $W > 0$ indicates the presence of genuine 3-party entanglement, whereas for $W \leq 0$ a definitive conclusion cannot be made. We thus define $W = 0$ in this case. The criterion W is basis-dependent. Numerically, we thus maximize its value over all possible local unitary transformations $(U_1 \otimes U_2 \otimes U_3)\rho(U_1^\dagger \otimes U_2^\dagger \otimes U_3^\dagger)$, where U_j is a generic 2×2 unitary matrix for the spin j . While it is not an entanglement quantifier, large values of W generically correspond to stronger genuine 3-party entanglement. For instance, W is maximal for Werner states, which are maximally-entangled 3-qubit states, and is minimal for the maximally mixed state (the identity).

B. TEST OF THE FULL-RANK HYPOTHESIS

We test the full-rank hypothesis (FRH) for the icosahedral molecule at $h = 3$ for three adjacent sites. In Fig. S1 we plot the minimal eigenvalues λ_{\min} of the 3-spin reduced density matrices for each eigenstate of the Hamiltonian, labelled by the corresponding energy E . All the minimal eigenvalues are strictly positive, which indicates that the FRH is satisfied. The smallest λ_{\min} occurs in the groundstate.

C. PHASE DIAGRAM OF THE MOLECULAR QUANTUM MAGNET

We report the zero-temperature connected correlation functions of adjacent spins in the anti-ferromagnetic Ising model on the icosahedral molecule as a function of the transverse field h , see Fig. S2. By symmetry we have $\langle \sigma^{x,y} \rangle = 0$. The point $h = 3$ corresponds to a generic point of the phase diagram.

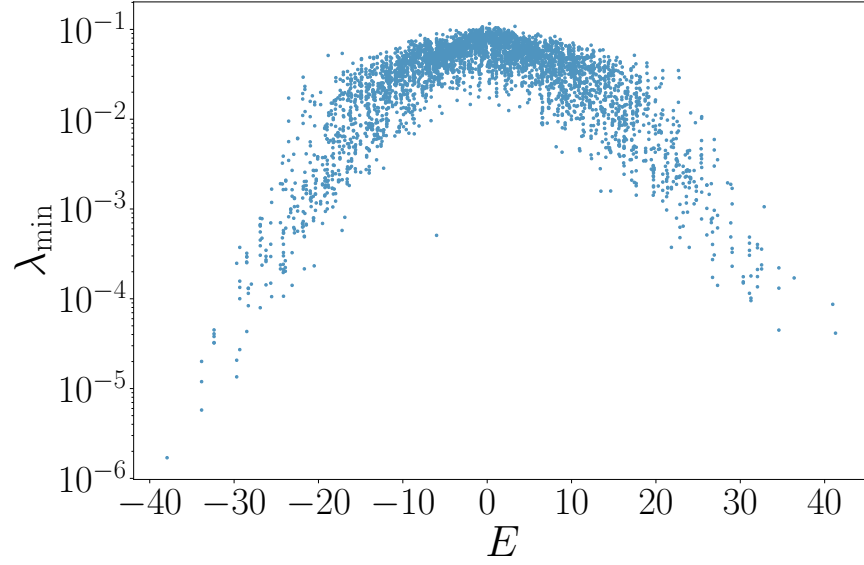


FIG. S1. **Test of the full-rank hypothesis.** Minimal eigenvalue λ_{\min} of the reduced density matrices for three adjacent spins in the icosahedral molecule at $h = 3$ for the whole spectrum, labelled by the corresponding energy E .

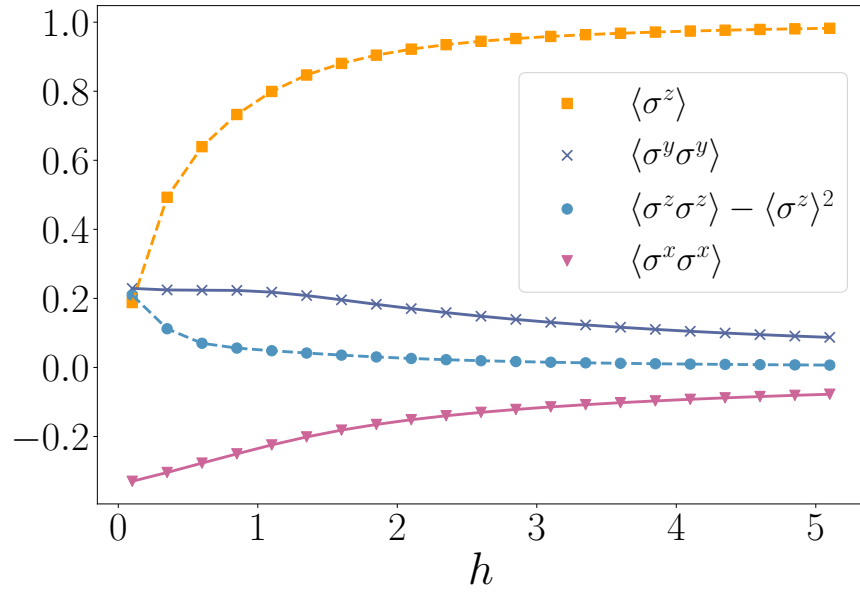


FIG. S2. **Spin correlations in the icosahedral molecule.** Various spin correlation functions versus the transverse field in the icosahedral molecule at zero temperature.

D. DETAILS ON THE QUENCH PROTOCOL

In the quench protocol, we initialise the system in a pure product state of up and down spins, and let it evolve under the Ising Hamiltonian discussed above with $h = 3$. We illustrate the initial state in Fig. S3. This is a planar representation of the icosahedral molecule, where blue sites are initialised in a spin-up state, whereas orange one are initialised in a spin-down state. The coloured face represents the 3-spin subsystem for which we compute \mathcal{D} and W during the time evolution.

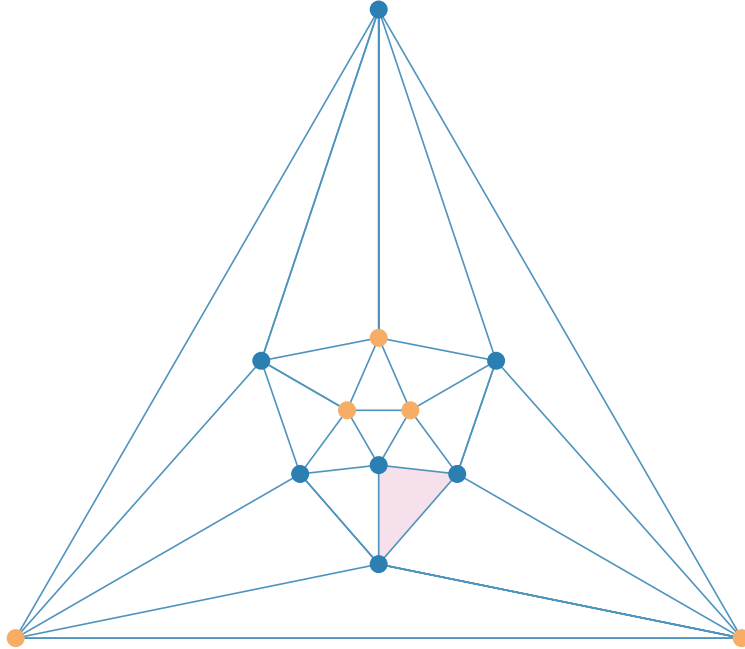


FIG. S3. **Initial state in the quench protocol.** Blue sites are initialised in a spin-up state, whereas orange one are initialised in a spin-down state. We focus on the coloured face during the time evolution.